Waste and Biomass Valorization (2021) 12:2283–2302
https://doi.org/10.1007/s12649-020-01175-2

ORIGINAL PAPER

Effect of Probe Ultrasonication, Microwave and Sunlight on Biosynthesis, Bioactivity and Structural Morphology of *Punica granatum* Peel's Polyphenols-Based Silver Nanoconjugates

Rimpi Foujdar[1] · Harish Kumar Chopra[2] · Manav Bandhu Bera[1] · Anil Kumar Chauhan[3] · Palak Mahajan[1]

Received: 2 April 2020 / Accepted: 14 July 2020 / Published online: 22 July 2020

Abstract
Biosynthesis of silver nanoconjugates using agro-waste has drawn the attention of the researchers in recent years due to eco-friendly and low-cost methods. A comparative study on various techniques (sunlight, probe ultrasonication, and microwave irradiation) of silver-bio-nanoconjugate production was carried out using lyophilized pomegranate peel polyphenols. Polyphenols from pomegranate peel extract were identified by LC–MS. The reaction time of each technique for the synthesis of pomegranate peel's polyphenols-based silver nanoconjugates was optimized by UV–visible spectroscopy, dynamic light scattering, and antioxidant activity. Further, they were characterized by FT-IR spectroscopy, XRD, FESEM–EDX, elemental mapping, TEM, and zeta potential. UV-spectroscopy and DLS results showed that the sunlight, probe ultrasonication, and microwave irradiation technique could reduce silver (Ag+) ions to silver nanoparticles (Ag0) at λ max ~ 420 nm with Z-average diameters 51.63–94.76, 40.51–61.47, and 43.40–66.52 nm, respectively. The antioxidant activity was maximum at 50 s of microwave irradiation treatment followed by 15 min of probe ultrasonication and 20 min of sunlight exposer. However, TEM analysis revealed that the probe ultrasonication treated nanoconjugates were spherical, smaller, and less aggregated. FT-IR spectra confirmed the involvement and conjugation of various functional groups from pomegranate peel polyphenols. Probe ultrasonic-assisted-silver nanoconjugates showed good antibacterial activity against *S. aureus* and *E. coli* as compared to microwave-assisted silver nanoconjugate.

✉ Manav Bandhu Bera
drmbbera@yahoo.com

[1] Department of Food Engineering and Technology, Sant Longowal Institute of Engineering and Technology, Longowal, Punjab 148106, India

[2] Department of Chemistry, Sant Longowal Institute of Engineering and Technology, Longowal, Punjab 148106, India

[3] Department of Dairy Sciences Food Technology, Institute of Agricultural Sciences, BHU, Varanasi 221005, India

Graphic Abstract

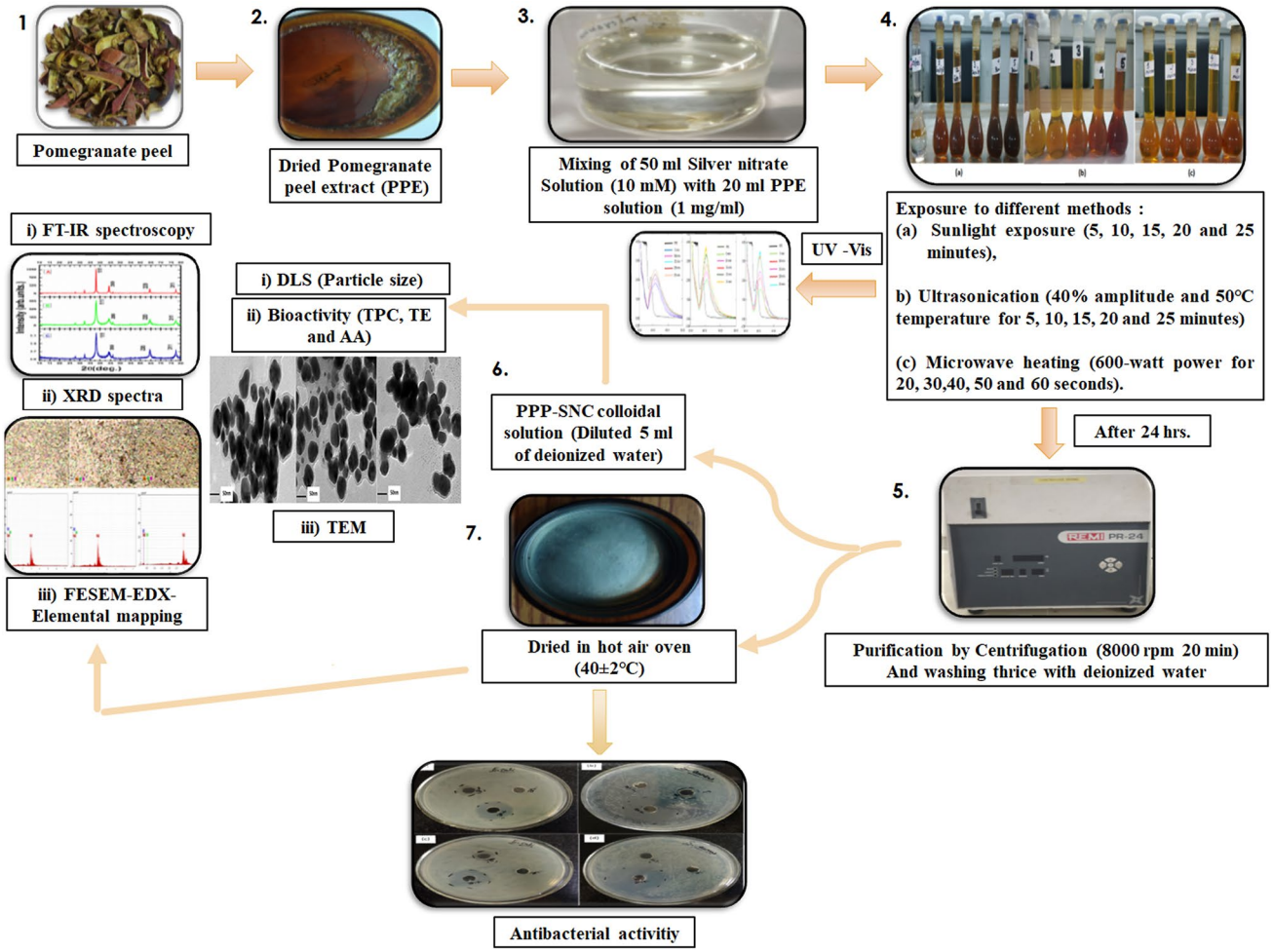

Keywords Pomegranate peel polyphenol · Probe ultrasonication · Silver nanoconjugate · Liquid chromatography–mass spectroscopy · Antioxidant activity · Antibacterial activity

Abbreviations

AA	Antioxidant activity
DPPH	2,2-Diphenyl-1-picrylhydrazyl
EDX	Energy dispersive X-ray
FESEM	Field emission scanning electron microscope
FTIR	Fourier-transform infrared
HHDP	Hexahydroxydiphenoyl
LCMS	Liquid chromatography–mass spectroscopy
PPP	Pomegranate peel polyphenol
PPP-SNC	Pomegranate peel polyphenol-based silver nanoconjugate
TE	Total ellagitannin
TEM	Transmission electron microscope
TPC	Total phenolic content
UV–vis	Ultraviolet–visible
XRD	X-ray diffractometer
ZOI	Zone of inhibition

Statement of Novelty

Pomegranate peel contains valuable polyphenol is considered too wasteful in the absence of suitable techniques of value addition. However, the utilization of pomegranate peel in the biosynthesis of silver nanoconjugates is a zero-waste strategy that could support the green technology campaign. Probe ultrasonication-assisted greener-synthesis of silver is proved as a simple, eco-friendly and efficient technique to produce well structured, pomegranate peel polyphenol silver nanoconjugates having high antioxidant and antimicrobial properties which would find application in the field of

biomedical as well as food preservation including designing of the novel food packaging system and postharvest management of fruits and vegetables.

Introduction

Nanoparticles have gained special attention recently given their unique physical, chemical, and optical properties. Characteristic properties are due to the very small size of particles (10^{-9}) having a high surface area to volume ratio and show efficient behavior even at a very lower concentration [1, 2]. Due to its nano size, it can penetrate the cells and help in delivering the drug on the specific site.

Application of nanotechnology in health, food, and agriculture has been well recognized especially in antimicrobial based food packaging, formulation of nano-preservatives, delivery of nanomedicine/drugs and nutraceuticals, vectors for gene delivery, nano-imaging and biosensors [2, 3].

Metal nanoparticles have been synthesized using chemical reducing agents [4], ultrasonication [5], UV- ray exposure [6] microwave irradiation [7], the ionic-liquid supported method [8], gamma rays [9] and biological methods [10], etc. Nano-silver is one of the metallic nanoparticles with the highest degree of commercialization [1]. The majority of the methods used for metallic nanoparticle production involve expensive and toxic chemicals that restrict its use in the synthesis of nanoparticles. To overcome these drawbacks, the research has been focused on the biological synthesis of nanoparticles. Numerous studies have been reported on the synthesis of nano-silver using plant extract and microorganisms [11–17]. The mechanism governing the production of biosynthesized nanoparticles is the conjugation of silver ions with various biomolecules to achieve the reduction of Ag+ to Ag0. The conjugation of plant polyphenols with metal nanoparticles exhibit the advantageous properties of both the materials [18]. The polyphenol not only acts as a reductant and capping agent during the synthesis of metallic nano-particles but also enhances the antioxidant activity of nanoparticles whereas conjugated silver nano-particles improve the stability of polyphenols under adverse conditions (such as heat, light, etc.).

Toxicity of silver nanoparticles towards cell is the main safety concern which prohibits its application. Although many studies already claimed that low concentration (5–250 µg/ml) of biosynthesized nanoparticles are non-toxic towards normal cells while toxic for cancer or bacterial cells [19–22]. Khorami et al. [21] studied cell cytotoxicity of wall nut green husk extract-based silver nanoparticles against tumor cell lines (MCF-7) and normal cell lines (L-929). They observed that biosynthesized nanoparticles showed 15% maximum cell death for the normal cell after 48 h. whether commercial chemical synthesized silver nanoparticles showed 60% cytotoxicity towards normal cells. On the contrary silver nanoparticles showed superior cytotoxic effect against cancer cells. It was reported that the combined effect of silver nanoparticles and polyphenols not only increased the ROS generation but also inhibited the transcription process. The antioxidants compounds such as polyphenols exhibit toxicity only against the non-healthy cell. In a conclusion of the above discussion polyphenol-rich plant extract-based silver nanoparticles exhibit a better result in the direction of cell cytotoxicity either normal or carcinogen cells as well as bacterial cells.

Various plant extracts are used for the synthesis of silver nanoparticles which includes the use of agro-waste derived from bark, lemon, grape, and orange processing industries. Utilization of agro-waste for the above purpose is an attractive approach due to its low cost and a resourceful alternative for waste minimization [23–27]. Pomegranate peel extract was reported as one of the most powerful agro-waste having high antioxidant activity and potential for green synthesis of silver nanoparticles [28, 29]. Polyphenols are responsible mainly for the reduction of silver ions which trigger the synthesis of silver nanoparticles [30].

Despite their crucial involvement in the synthesis of silver nanoconjugate, reports on the efficient production of pomegranate peel extract assisted silver nanoparticles are scarce. A few reports are available wherein the silver nanoparticles have been synthesized using an incubation shaker for 24 h and magnetic stirrer. They characterized the synthesized silver nanoparticles by UV-spectra, FT-IR, SEM, and antibacterial activity [31, 32]. However, few reports claimed that a combination of physical and biological techniques produce more uniform and stable nanoparticles [19, 33–35] in a short duration.

Cultivars are another factor that significantly affects the synthesis of silver nanoparticles and their bioactivity [36, 37]. Matties et al. [36] observed that leaves of two cultivars (*Leccino* and *Carolea*) belonging to the species of *Olea Europea* produce different shapes and sizes of nanoparticles. Their anticancer and antibacterial properties are also varied. Therefore, the use of specific variety for the production of silver nanoparticles would be aid beneficial for a particular study. In our previous study, it was already reported that *Bhagwa* variety pomegranate peel is a powerful source of antioxidant as compared to other cultivars [28]. As a continuation of our previous study hereby we report the bioinspired synthesis of silver nanoparticles using specific (*Bhagwa*) variety of pomegranate peel. Additionally, in the current study first time, comparative studies on three different nano-conjugation techniques were carried out using pomegranate peel polyphenol (PPP) and exposing the reaction in the presence of sunlight, microwave irradiation, and probe ultrasonication. Initially, the time of exposer was optimized for the synthesis of pomegranate

peel polyphenol-silver nano-conjugate (PPP-SNC) using three approaches based on visual observation, UV spectral analysis, DLS, and bioactivity (TPC, TE, and AA). Further, nanoconjugates were characterized using FESEM–EDX, Elemental mapping, TEM, XRD, FT-IR spectroscopy, and Zeta potential. Antimicrobial activity was also studied.

Materials and Chemicals

Silver nitrate was collected from Merk Life Science Private Limited (Mumbai). *Bhagwa* variety's pomegranates were collected from the garden of Sholapur, Maharashtra in August 2019. Deionized water (Merck Millipore ultrapurification system, M Progard TS2) was used throughout the study of extraction, synthesis, and purification. All the chemicals were used analytical grade and HPLC grade solvent used for LCMS study.

Extraction of Polyphenols from Pomegranate Peel

Peels were separated from fruits and washed with deionized water. The peels were shredded and tray dried at 40 ± 2 °C until the moisture reaches < 5% on a wet basis. Peels were ground and passed through a sieve (60 B.S.S mesh size). Polyphenols from pomegranate peel powder were extracted according to the method of Foujdar et al. [28]. Purified samples were lyophilized and used for further analysis.

Liquid Chromatography–Mass Spectroscopy (LC–MS)

Identification of phenolic compounds of the lyophilized sample was done using LC–MS (Waters, Micromass Q-TOF micro) having X- bridge waters C-18 column (4.6*250 mm length, 5 µm diameter). The experiment was performed by following the described method of Seeram et al. [38]. Solvent A (2% acetic acid/water), B (2% acetic acid/ methanol) was used throughout the study. The volume of injection was 20 µl and the flow rate was 0.8 ml/min. Mass spectra were recorded at electron spray negative mode with a scan range of 120–1500 amu. Presence of compounds in each peak of the mass spectra was identified by matching their molecular ions $[M\text{-}H]^{-1}$ from the standard mass spectra and available literature data [39–41].

Synthesis of Pomegranate Peel's Polyphenols-Based Silver Nanoconjugate (PPP-SNC)

PPP-SNC was prepared by following the method [42] with modification. Briefly, 50 ml of silver nitrate (10 mM) was mixed with 20 ml of extract (1 mg of dry weight extract/ml of deionized water). Three different techniques were used for the synthesis of silver nanoconjugate namely sunlight exposure (5, 10, 15, 20 and 25 min), probe ultrasonication at fixed an amplitude (40%) and temperature (50 °C) for 5, 10, 15, 20 and 25 min and microwave irradiation at 600-W power for 20, 30, 40, 50 and 60 s. After treatment, the beaker containing the mixture was covered with aluminum foil and kept for 24 h at room temperature. The reduction of silver nitrate to PPP-SNC was initially observed visually by colour change. The UV–Vis spectrophotometer (Shimadzu, UV-1800, Malaysia) was used to check the variation of absorbance spectra of synthesized nanoconjugates. The PPP -SNC was separated by centrifugation (REMI-PR 24) at 8000 rpm for 20 min and purified by washing three times with deionized water following centrifugation (8000 rpm for 15 min). The precipitate of silver nanoconjugates was further dispersed in 5 ml of deionized water and analyzed for particle size, total phenolic compound, total ellagitannin, and antioxidant (DPPH scavenging) activity.

Bioactivity Study of PPP-SNC

Total Phenolic Content

TPC was quantified by using the method described by Kazemi et al. [43] using a spectrophotometer (HACH, DR-6000 Model) at 765 nm wavelength with slight modification. The modification included as 1 ml colloidal solution was added into 5 ml of FCR reagent (tenfold dilution) and 4 ml of sodium carbonate solution (7.5%). The TPC was expressed in terms of µg Gallic acid equivalent (GAE)/ml of silver nanoconjugate solution.

Total Ellagitannin

Total Ellagitannins (hydrolysable tannins) were determined using the method described by [29]. Results were expressed as µg Tannic acid equivalent (TAE) per ml of silver nanoconjugate solution.

Antioxidant (DPPH Scavenging) Activity

The spectrophotometric method described by [43] was followed for the analysis of the free-radical scavenging activity of PPP-SNC using 2,2-diphenyl-1-picrylhydrazyl (DPPH). 1 ml of nano colloidal solution was added into 3.9 ml of DPPH activity. Absorbance was taken at 517 nm wavelength. Scavenging % was calculated by following the equation:

$$\text{DPPH scavenging } (\%) = [(A - B)/A] \times 100,$$

where 'A' and 'B' is the absorbance of control and sample.

Comparative Study Between Peel Extract and PPP-SNC on Antioxidant Compounds

To conduct a comparative study between extract and PPP-SNC on TPC, TE, and AA, the same sample concentration (dry weight basis) was used. The sample was dissolved into dimethyl sulfoxide (DMSO). The method was performed as described by our previous study [28].

Characterization of PPP-SNC

UV–Vis Spectrophotometer

Reduction and conjugation of silver ions to PPP-SNC were observed by ultraviolet–visible spectrophotometer (Shimadzu, UV-1800, Malaysia). UV–Vis spectra of samples were taken in the wavelength range between 200 and 800 nm.

Dynamic Light Scattering (DLS)

Particle size and zeta potential were measured by dynamic light scattering technique (Malvern-Zetasizer Instrument). The temperature of the cell was maintained at 25 °C.

Fourier Transform Infrared (FT-IR)

FT-IR study was performed by Fourier transform infrared-spectroscope (Perkin Elmer, USA) to determine which functional group of pomegranate peel polyphenol responsible for reduction and conjugation of PPP-SNC. In FT-IR spectra analysis, a small amount of hot air oven-dried sample (at 37 ± 3 °C temperature) was used to form KBr pellet, and spectra were recorded in between 4000 and 400 cm^{-1} infrared range with a resolution of 4 cm^{-1}.

X-Ray Diffractometer (XRD)

XRD (BRUKER, D-8 Advance) equipped with K αCu radiation generator ($\lambda = 1.5419$ Å) and nickel monochromator was used to obtain X-ray pattern at 30 kV and 100 mA. The scanning was recorded in the region of 2θ from 10° to 90°. The crystal size of nanoparticles was calculated by Scherer's equation [44]:

$$D = K\lambda\beta \ \mathrm{Cos}\,\theta,$$

where D is the average crystal size, K is the Scherer coefficient (0.89), λ is the wavelength of X-ray (1.5406 Å), β is the full width at half maximum and θ is Bragg's angle (2θ).

Field Emission Scanning Electron Microscopy (FESEM)–Energy Dispersive X-Ray (EDX) with Elemental Mapping

Morphology of the PPP-SNC was analysed by FESEM (Ultra High Resolution, scanning electron microscope SU8010, Hitachi Model). The dried powder sample was mounted on a carbon-coated copper grid. EDX and elemental mapping were accomplished by FESEM equipped with EDX and elemental mapping attachment.

Transmission Electron Microscopy (TEM)

The internal morphology of the PPP-SNC was obtained by TEM (Hitachi, model H-7650) image analysis using an accelerating voltage of 80 kV emitted at 11.8 μA.

Antibacterial Activity of PPP-SNC

The antibacterial activity of synthesized PPP-SNC was evaluated by agar well diffusion method [42]. Two food poisoning bacteria namely, *Staphylococcus aureus*-gram positive (MTCC-3160) and *Escherichia coli*- gram-negative (MTCC-452) were used in the study. All the nanoconjugates were dissolved in DMSO at a concentration of 5 mg/ml. Tetracycline (50 μg) used as a positive control and DMSO as a control. Zone of inhibition measured in mm after incubation at 37 °C for 24 h.

Statistical Analysis

The data have represented the average of three readings. One way-analysis of variance (ANOVA) with Duncan's multiple range test (Software SPSS 253 16.0) was used to determine significant differences at $P < 0.05$ among the mean values.

Results and Discussion

Identification of Polyphenols from Pomegranate Peel Extract Using LCMS

Chromatogram of pomegranate peel polyphenols showed nine major peaks (Fig. 1). Mass spectra and fragmentation patterns were used to identify the peaks. Peak 1 was identified as galloyl hexoside where one single fragment found in mass spectra at m/z 331.09 (Table 1). Compound eluted at 8.29 min produced a molecular ion at m/z 331.10 $[M\text{-}H]^{-1}$ and a characteristic fragment ion at m/z 271. Compound at (Peak 2) was identified as galloyl hexoside.

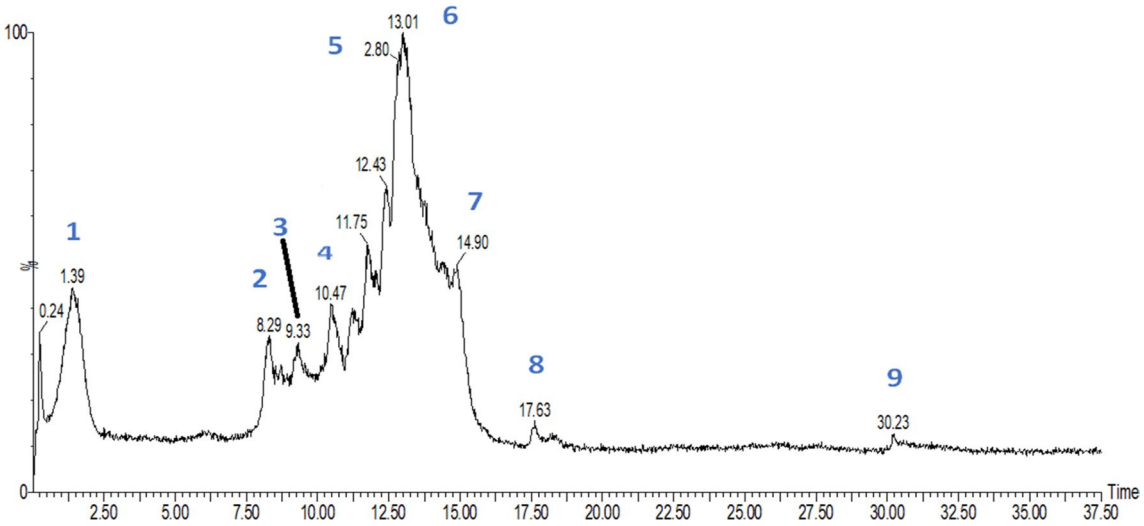

Fig. 1 Chromatograph of lyophillized pomegranate peel extract

Table 1 Identification of polyphenol compounds from pomegranate peel extract using mass spectra

Peak no.	Retention time (min)	Compound name	Molecular weight $[M-H]^{-1}$	Fragment pattern (M/Z)
1	1.39	Galloyl hexoside	331	331.09
2	8.29	Galloyl-hexoside	331	331.09, 271.06
3	9.33	Digalloyl-hexoside	483	483.12, 481.11, 331.10, 271.06
4	10.47	Galloyl-HHDP-hexoside	633	633.13, 541.09, 331.10, 271.07
5	12.80	Punicalagin α	1083	1083.19, 783.17, 707.15, 541.09, 483.13
6	13.01	Punicalagin β	1083	1083.22, 783.17, 707.15, 633.15, 541.09, 483.14, 301.03
7	14.90	Pedunculagin I isomer	783	783.16, 481.12, 331.10
8	17.63	Pedunculagin I isomer	783	783.20, 481.12, 331.10
9	30.23	HHDP-hexoside	481	481.12, 275.84

Peak 3 eluted at 9.33 has $[M-H]^{-1}$ ion at m/z 483.12 and a strong fragment ion at m/z 331.10 and identified as digalloyl hexoside. Similar characteristics fragment ion was reported [40, 41] in pomegranate juice and identified as digalloyl hexoside. Peak 4 eluted at 10.47 min has a deprotonated ion at m/z 633.17 $[M-H]^{-1}$ and product ion at m/z 541.09, 331.10, and 271.07. The fragment pattern of this study was different from the existing literature data [39–41]. But the presence of punicalagin isomers (m/z 541.09) and galloyl hexoside (m/z 331.09) indicated that this compound should be galloyl-hexahydroxydiphenoyl-hexoside. This compound was identified in pomegranate flower polyphenols by [39]. Peak 5 and 6 eluted at 12.80 and 13.01 min was accounted for punicalagin α and β (Table 1). This compound was confirmed by comparing with standard retention time and mass spectra. Peak 6 has a molecular ion at m/z 1083.22 $[M-H]^{-1}$. The fragment ions were found at m/z 783.17, 707.14, 633.15, 541.09, 483.14, and 301.03 and matched with the fragment pattern of standard (punicalagin). Retention time and fragment pattern of standard conferred the presence of punicalagin β. Peak 5 has also a production at 1083.19 $[M-H]^{-1}$ which showed a similar fragment pattern. Based on existing literature [39] and reference of the standard this compound was identified as punicalagin α. Punicalagin is the main ellagitannin compound of pomegranate peel identified by Seeram et al. [38] during a large scale of purification of ellagitannin from pomegranate peel. Peak 7 and 8 have a deprotonated ion at $[M-H]^{-1}$ m/z 783.16 and 783.20 and a production at m/z 331.10 (galloyl hexoside) and 481.12 (di galloyl hexoside). This peak was identified as (Penduculagin I isomers). Each of the two different retention times resembled the isomeric structure. These compounds were also reported by Fischer et al. [40]. Peak 9 had deprotonated ion at $[M-H]^{-1}$ 481.12 which was assigned for

HHDP-hexoside (Fig. 1, Table 1). A similar compound was identified in *Punica granatum* L. Juice by Mena et al. [41].

Synthesis of Pomegranate Peel's Polyphenols-Based Silver Nanoconjugate (PPP-SNC)

Visual Observation and Spectral Analysis

Visual observations of PPP-SNC were confirmed by a colour change from yellow to dark brown (Fig. 2a–c). The colour intensity increased with the increase in exposure time for all three methods. However, there is a marked increase in the colour under sunlight exposure. Change of colour indicates the formation of silver nano-conjugates [15, 45, 46]. In line with the colour changes, the reduction of silver ions into nanoconjugate was further evaluated by UV visible spectroscopy. Spectral analysis showed that all nanoconjugates have maximum absorbance near about 420 nm whereas peel extract showed maximum absorbance spectra at 370 nm (Fig. 3a–c). The λ_{max} of all the treated silver nanoconjugate samples were respectively for sunlight (433.5–429 nm), probe ultrasonication (424–415 nm), and microwave (421.5–410 nm) wavelengths. However, several literatures reported that the nanoparticles showed a spectral wavelength range of 220–800 nm [25, 32, 47–49]. It has been observed that absorption spectra were influenced by the shape, size, and morphology of nanoparticles. The characteristic peak of nano-silver is mainly due to surface plasmon resonance which indicates the formation of silver nanoparticles. It was observed that the absorbance of all nanoconjugates increased with increasing time of exposure (Table 2). The wide absorbance peaks indicate a larger particle size [50]. The Fig. 2b and c showed that probe ultrasonication and microwave irradiation treated PPP-SNC have smaller peak area and hence smaller particle size as compared to the large peak area of sunlight treated PPP-SNC sample

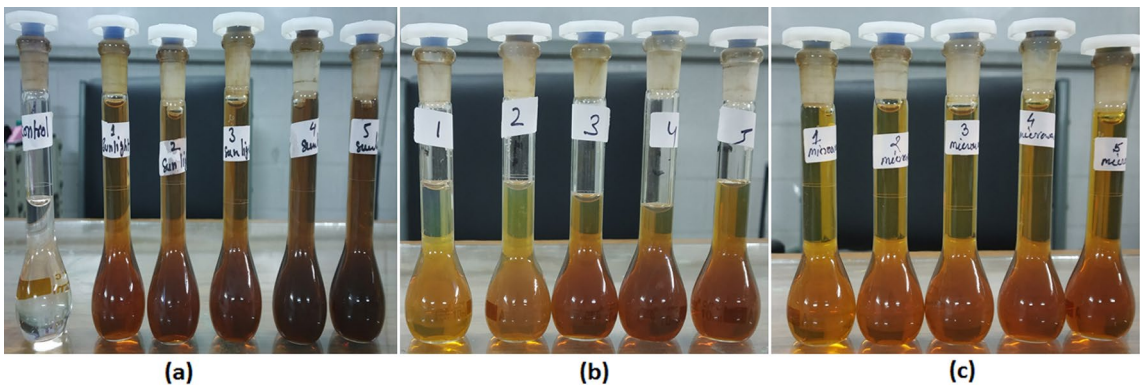

Fig. 2 Visual observation of **a** sunlight, **b** probe ultrasonication and **c** microwave based PPP-SNC

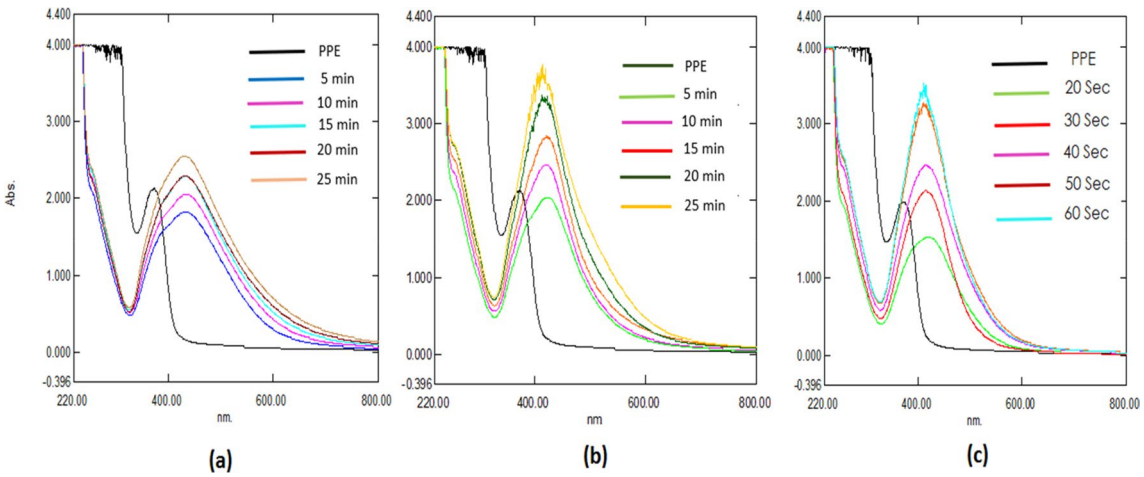

Fig. 3 UV-spectra of **a** sunlight, **b** probe ultrasonication and **c** microwave based PPP-SNC

Table 2 UV–vis spectroscopy results of PPP-SNC using three different techniques

Sl. no.	Techniques	Time (min)	Maximum wavelength (nm)	Maximum absorbance
1	Sunlight	5	432	1.826
		10	433.5	2.057
		15	433.5	2.296
		20	431.5	2.293
		25	429	2.56
2	Probe ultrasonication	5	424	2.041
		10	421	2.477
		15	424.5	2.841
		20	423.5	3.357
		25	415	3.765
3	Microwave	5	415	2.132
		10	421.5	1.532
		15	413	2.476
		20	410	3.286
		25	410.5	3.548

Table 3 Effect of time and techniques on the particle size of PPP-SNC

Sl. no.	Methods	Time	Particle size (Z-average diameter in nm)
1	Sunlight	5 min	94.8
2		10 min	86.2
3		15 min	85.3
4		20 min	51.6
5		25 min	90.5
6	Probe ultrasonication	5 min	49.8
7		10 min	41.7
8		15 min	40.5
9		20 min	52.2
10		25 min	61.5
11	Microwave irradiation	20 s	66.5
12		30 s	53.9
13		40 s	59.1
14		50 s	43.4
15		60 s	46.3

(Fig. 2a). This result was further confirmed by DLS, FESEM with EDX, and TEM.

Effect of Exposure Time PPP-SNC Synthesis on the Particle Size

The particle size of PPP-SNC varied respectively for sunlight (51.63–94.76 nm), probe ultrasonication (40.51–61.47 nm), and microwave irradiation (43.39–66.52 nm). The particle size of sunlight, probe ultrasonication, and microwave irradiation treated PPP-SNC decreased with increasing exposure time (Table 3). Reduction in the particle size with an increase in the incubation time could be attributed to the fact that time needed to react the polyphenols on the silver nitrate for reduction of silver ions to nanoparticles was available. On the other side, an increase in the time beyond 20 min, 15 min, and 50 s for sunlight, probe ultrasonication, and microwave irradiation caused aggregation of particles hence the particle size increased. Similar report on agglomeration was discussed by Fatimah and Indriani [51]. Another reason for the increase of the particle size with extending the probe ultrasonication time could be due to high amplitude and longer probe ultrasonication led to the formation of free radicals and destabilization of the PPP-SNC by intramolecular regrouping and depolymerization of the molecules [52]. These results were in line with the UV–vis study of PPP-SNC reported earlier. A similar result was reported by Guzmán et al. [7] who found that particle size of gallic acid-chitosan modified silver nanoparticles was larger at 20 min (54.90 ± 64.8 nm) than 10 min of probe ultrasonication (39.78 ± 13.2 nm) exposure. In the case of microwave irradiation, initially, the particle size is reduced with irradiation time (20–50 s) since irradiation can easily penetrate the reaction solution and produce heat homogenously, giving rapid crystal growth and uniform nucleation [53]. Further, increasing the irradiation time beyond 50 s the particle size was increased because irradiation time is directly proportional to temperature. As time increases the temperature of solution reach nearly about boiling temperature which causes degradation of the stabilizing molecules present in the plant extract. The stabilizing molecules help to prevent the aggregation by making a layer around the surface of nanoparticles. Degradation of these molecules results in agglomeration of particles subsequently led to the formation of large particles. A similar observation was reported by Kazemzadeh et al. [54]. As they observed that increasing microwave irradiation exposure, initially it reduced the particle size and beyond 75 s larger agglomerated particle size obtained.

Effect of Exposure Time PPP-SNC Synthesis on TPC, TE, and AA

The antioxidant activity of synthesized nanoconjugates depends on the properties of various polyphenolic components attached to their surface. The effect on the exposure time of different techniques used for the synthesis of PPP-SNC on TPC, TE, and AA are represented in Fig. 4a–c. The results indicated that exposure time has a significant effect on TPC, TE, and AA of synthesized PPP-SNC for each technique. It was found that the TPC, TE, and AA of synthesized silver nanoconjugates increased significantly with

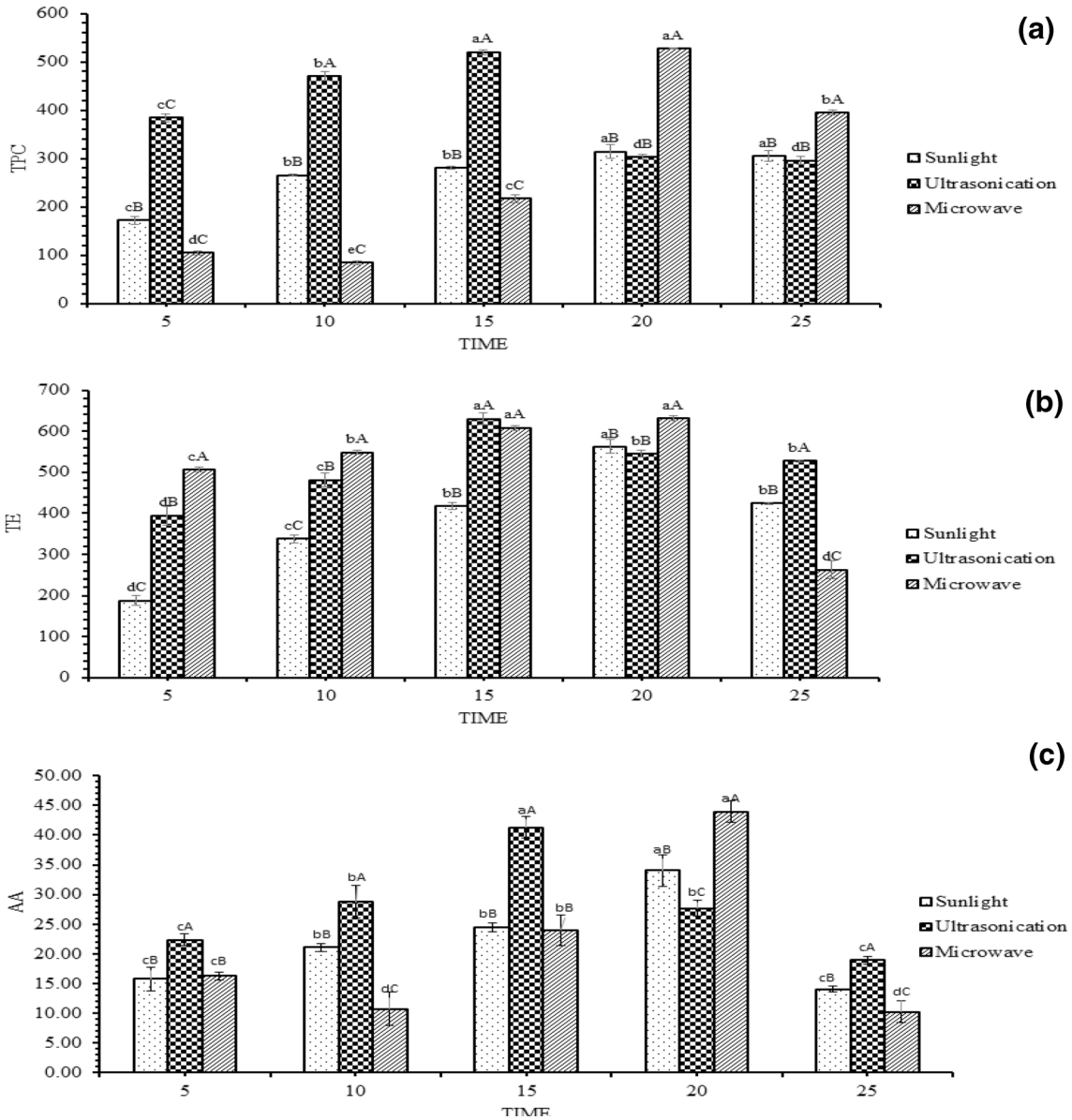

Fig. 4 Effect of time (5–25 min for sunlight and probe ultrasonication and 20–60 s for microwave) for the synthesis PPP-SNC using different techniques on **a** TPC (μg GAE/ml), **b** TE (μg/TAE/ml) and **c** AA (% of DPPH scavenging). Different lowercase letter superscript in the column graph represent significant differences ($p \leq 0.05$) between the time of a particular technique. Different uppercase letter superscript in the column graph represent significant differences ($p \leq 0.05$) between different approaches

increasing the sunlight exposure time (314.49 ± 14.91 μg GAE/ml, 562.0 ± 16.75 μg TAE/ml, 34.02 ± 2.69% of DPPH scavenging) up to 20 min thereafter a significant reduction (12.91% of TPC, 24.55% of TE, 41.97% of AA) was observed (Fig. 4a). In the case of probe ultrasonic exposure, the maximum TPC, TE, and AA of PPP-SNC were found at 15 min. Similarly, 50 s of microwave irradiation gave maximum values of TPC, TE, and AA (Fig. 4b–c). Further increase in exposure time the antioxidant activity significantly reduced. It may be due to increasing the time of exposure irrespective of the process followed, degradation and structural changes of polyphenols might have occurred which led to the reduction in antioxidant activity. PPP-SNC prepared by following the probe ultrasonication and microwave process exhibited enhanced antioxidant compounds (Fig. 4). It may be due to the functional group of pomegranate peel polyphenol attached/conjugated to the surface of silver nanoparticles which enhanced the antioxidant effect of PPP-SNC [55].

Table 4 Comparative study of antioxidant activity of PPP-SNC with pomegranate peel extract

Sl. no.	Sample name	TPC (mg GAE/g of sample)	TE (mg TAE/g of sample)	Antioxidant activity (% of DPPH scavenging activity)
1	Pomegranate peel extract	350.41 ± 7.75^{a}	325 ± 9.42^{a}	92.03 ± 0.69^{a}
2	Sunlight assisted PPP-SNP	179.48 ± 14.28^{c}	186.67 ± 9.10^{c}	43.78 ± 1.88^{c}
3	Ultrasonication assisted PPP-SNC	211.85 ± 10.82^{b}	221.33 ± 11.47^{b}	50.26 ± 2.39^{b}
4	Microwave assisted PPP-SNC	212.47 ± 7.90^{b}	223.67 ± 11.09^{b}	52.98 ± 1.34^{b}

Results are expressed as average values ± standard deviations (n = 3). Different letters superscript in the column represents significant differences ($p \leq 0.05$)

Comparative Study on Antioxidant Activity of Extract and Silver Nanoparticles

Table 4 represents a comparative study of TPC, TE, and antioxidant activity between extract and silver nanoparticles obtained from three different methods at a constant time (20 min, 15 min and 50 s for sunlight, ultrasonication and microwave irradiation time). It was revealed that the TPC and TE are maximum in the extract as compare to silver nanoconjugates. Phenolic and ellagitannin compounds have been reported as the most important compounds which are responsible for antioxidant capacity in pomegranate peel extract [56]. Therefore, the higher amount of TPC and TE in PPP can be taken as a fine indication of its higher antioxidant ability. Similar results were recorded by Mahendran and Kumari [57], who observed that TPC and total tannins were higher in *N. nimmoniana* fruit extract than silver nanoparticles. A parallel result was also observed in *Iresin herbstii* leaf extract assisted silver nanoparticles [58]. The results of TPC and TE are in line with the results of DPPH scavenging activity. The silver nanoparticles showed a good antioxidant activity but lower than extract. It was reported that the antioxidant activity of synthesized nanoparticles is due to the conjugation of phenolic compounds which showed a deleterious effect against free radicals [59]. Our results are in agreement with the results of Mahendran and Kumari [57]. They observed that *N. nimmoniana* fruit extract has a lower value of IC50 than silver nanoparticles. The lower value of IC50 indicates a higher antioxidant activity. A similar observation was also reported by Mittal et al. [59] in *Syzygium cumini* and Reddi et al. [60] in *Piper longum* fruit.

Characterization of Synthesized PPP-SNC Prepared by Different Techniques

As discussed earlier, it was observed that 20 min of sunlight, 15 min of probe ultrasonication, and 50 s of the microwave irradiation was suitable exposure time for the synthesis of PPP-SNC and the same samples were used for further characterization to find out the efficiency/effectiveness of these techniques.

FT-IR Spectroscopy

The Fourier transform infrared spectroscopy (FT-IR) is used to identify the possible phenolic compounds responsible for conjugation and reduction of metallic nanoparticles synthesized by PPP. The FT-IR spectra of PPP and PPP-SNC synthesized by three different processes (sunlight, probe ultrasonication, and microwave irradiation) are shown in Fig. 5a–d. The spectrum of peel extract showed a broad band at 3366 cm^{-1}, which is assigned to the stretching vibration of –C–O–H group. The small peak observed at 2997 and 2127.1 cm^{-1} is characteristic of the stretching vibration band of aliphatic C–H groups. A peak at 1727.9 cm^{-1} and 1612.12 are attributed to C=O stretching vibrations of the carbonyl group. The peaks observed at 1226.7 cm^{-1} are attributed to the stretching vibration band of O–H group. The peak at 1513.2, 1444.1, and 1347.6 cm^{-1} are assigned to the skeletal vibration of the aromatic ring. A band at 1062.1 cm^{-1} is attributed to stretching vibrations of C–OH groups and 875.9 cm^{-1} is assigned for isolated hydrogen in the benzene ring Fig. 5a. Similar FT-IR spectra of pomegranate peel extract are reported [29]. Apart from, this, FT-IR spectra of sunlight assisted PPP-SNC showed the sharpest peak at 3432.4 cm^{-1} and other peaks were obtained at 1623.0, 1384.8, 1055.4, 693.7 cm^{-1} respectively (Fig. 5b). The major peak of probe ultrasonic treated PPP-SNC was observed at 1384.1 cm^{-1} and other peaks were found at 3434.2, 2923.8, 1628.9 cm^{-1}, respectively (Fig. 5c). While a sharp peak was found at 1384.1 cm^{-1}, followed by 3462.5, 2924.2, 1626.9, 1032.7, 685.4 cm^{-1} respectively for microwave irradiated PPP-SNC (Fig. 5d). The comparison of the FTIR spectrum of peel extract and silver nanoconjugates revealed only a few changes in the position as well as the absorption band. The broadband appearing at 3432.4 cm^{-1} (sunlight), 3434.2 cm^{-1} (probe ultrasonication), and 3462.5 cm^{-1} (microwave irradiation) which are sifted from 3366 cm^{-1} (peel extract) assigned for OH stretching vibration. According to many reports, this peak confirmed the presence of phenolic hydroxyl groups which are responsible for reduction as well as

conjugation or capping agent of nanoparticle [30, 47]. The peaks located at 2923.8 and 2924.2 cm^{-1} shifted from 2927 (peak of extract) are attributed to methylene stretching vibrations of alkanes and aldehydes [49]. While peaks at 1623.0, 1628.9, and 1626.9 cm^{-1} shifted from extract peak at 1612.2 are due to carbonyl compounds indicates the presence of protein [16]. The strong peak at 1384.8, 1384.1, and 1384.1 cm^{-1} are related to stretching of nitro compounds (N=O), and at 1055.4 and 1032.4 cm^{-1} can be allocated to the stretching of amines (C–N) and C–OH. Many reports on plant extract-based silver nanoparticles are reported which suggested that the carbonyl group of amino acid residues (free amines, peptides, and cysteine) in proteins can bind with silver. FTIR analysis of PPP-SNC confirmed that some bioactive compounds of peel extract such as phenolic compounds, ellagitannin, alkaloids, and amino acids are responsible for the biosynthesis of silver nanoparticles from silver nitrate solution. LC–MS data has been already witnessed for the presence of ellagitannin and other phenolic compounds in the extract (Table 1).

XRD Analysis

The XRD spectra of synthesized PPP-SNC using sunlight, probe ultrasonication, and microwave is shown in Fig. 6a–c. The pattern of XRD spectra of synthesized PPP-SNC showed a sharp peak at 38.4°, 44.33°, 64.44°, and 77.42° for sunlight which slightly varied with probe ultrasonication (38.17°, 44.23°, 64.54° and 77.43°) and microwave (38.23°, 44.33°, 64.53° and 77.50°). The sharp peaks were corresponding to 111, 200, 220, and 311 diffraction patterns of the face-centered- cubic silver metal (ICSD file No. 98-005-3761), which is in agreement with the earlier reports [7, 19, 47]. The extra peaks around 27.80°, 32.23°, and 46.26° (sunlight), 27.84°, 32.27° and 46.27° (probe ultrasonication), and 27.97°, 32.29°, and 46.29° (microwave irradiation) assigned to the presence of bio-organic compounds on the particle's surfaces. These studies explained the fact that the polyphenol compounds of pomegranate peel extract can accelerate the reduction of silver ions to nanoparticles via conjugation. XRD- spectral peaks for PPP-SNC synthesized by microwave irradiation process showed low intensity due to the copious amount of polyphenols' layer in comparison to PPP-SNC synthesized by probe ultrasound and sunlight assisted techniques (Fig. 6). XRD-spectral peaks of PPP-SNC synthesized by sunlight exposure showed the highest intensity due to a thin layer of polyphenol compounds (Fig. 6a). The results are also supported by the results of the antioxidant activity of nanoconjugates which showed that microwave irradiation PPP-SNC has higher antioxidant activity followed by probe ultrasonication and sunlight (Fig. 4). PPP-SNC nanoparticles were calculated for its crystallinity (74.40, 63.90, and 62.30%) and crystal size (34.99, 14.24, and 14.3 nm) respectively for sunlight, probe ultrasonication, and microwave. Both the crystallinity and size of crystal of PPP-SNC prepared by sunlight exposure were higher in comparison other two processes.

FESEM–EDAX and Elemental Mapping

FESEM study demonstrated that all synthesized PPP-SNC have a spherical shape (Fig. 7). Whereas probe ultrasonication treated PPP-SNC showed uniform distribution of particles with spherical shape (Fig. 7) which is followed by microwave irradiated PPP-SNC (Fig. 7). Sunlight assisted PPP-SNC showed uneven distribution with large particles (Fig. 7). A similar shape of silver nanoparticles was observed by Sana and Dogiparthi [49] using FESEM.

EDX used to estimate the amount of silver present in synthesized PPP-SNC and are shown in Fig. 8a–c. EDX analysis indicated that probe ultrasonication based PPP-SNC has the highest amount of silver (79.61%) than microwave (71.41%) and sunlight (73.07%). The results of EDX were confirmed by elemental mapping which indicated that the silver particles of probe ultrasonication treated PPP-SNC were more densely arranged as compared to microwave and sunlight (Fig. 9a–c).

Transmission Electron Microscopy (TEM) of PPP-SNC

Images from TEM of synthesized PPP-SNC showed that all the synthesized silver nanoparticles have a roughly spherical shape and well dispersed (Fig. 10a–c). However, the probe ultrasonication process gave more homogeneously distributed and smaller particles as compared to the other two processes (Fig. 10b). The particle size (mean diameter) of crystalline PPP-SNC was 32 ± 3.84 nm (probe ultrasonication), 37 ± 5.58 nm (microwave irradiation), and 40 ± 5.69 nm (sunlight) respectively. The pattern of the crystalline size of PPP-SNC using three different techniques is aligned with the pattern of XRD results. Ultrasonication (14.24 nm) has a smaller particle size than microwave-based PPP-SNC (14.3 nm) followed by sunlight which showed a larger crystalline size (34.99 nm) among them. Although, the average crystalline size of synthesized PPP-SNC observed in TEM is almost large to the average particle size calculated by XRD using Scherrer's equation. Our findings are similar to the observation of Alsamhary et al. [61].

All the nanoparticles surrounded by a thin layer of capping agent which should be assigned as polyphenol compound. The results of TEM are supported by [19, 24, 48, 55]. However, to the best of our knowledge, there is no report available till date on the comparative morphological study of bionanoconjugates prepared by three techniques viz. sunlight, microwave irradiation and probe ultrasonication. The

morphological study revealed that probe ultrasonication has a positive effect on the synthesis of PPP-SNC. Many works of the literature suggested that probe ultrasonication is a high energy approach that efficiently produces non-aggregated nanoparticles following the principle of acoustic cavitation [33, 51, 62, 63].

Zeta Potential

The zeta potential of PPP-SNCs is shown in Fig. 11a–c. The average zeta potential of PPP-SNCs was for probe ultrasonication (− 25.0 mv), sunlight (− 20.8 mv), and microwave irradiation (− 11.4 mv). It was observed that the average zeta potential of probe ultrasonication PPP-SNC was higher than the other two processes. The high negative zeta potential value inferred the long period stability of silver nanoconjugates due to negative–negative charge repulsion [19, 25].

Yield of PPP-SNC

Probe ultrasonication process gave a maximum yield of PPP-SNC which is followed by sunlight and microwave (Table 5). Similar observations are reported where thermal and probe ultrasonication approach was used for the synthesis of silver nanoparticles and *Ficus carica* fruit [55]. Probe ultrasonication produces cavitation within the liquid system could be the reason for the higher yield of nanoparticles [46, 64].

Table 5 Yield of PPP-SNC using different techniques

Sl. no.	Techniques	Yield of PPP-SNC (mg/100 ml of solution)
1	Sunlight	5.120 ± 0.271^{b}
2	Probe ultrasonication	7.633 ± 0.485^{a}
3	Microwave	3.790 ± 0.574^{c}

Results are expressed as average values ± standard deviations (n = 3). Different letters superscript in the column represents significant differences ($p \leq 0.05$)

Anti-Bacterial Activity of PPP-SNC

On a comparison of the result obtained from different techniques used to the characterization of PPP-SNC, it has been observed that probe ultrasonication and microwave were capable of producing silver nanoconjugates with higher antioxidant activity and smaller particle size. Therefore, these two techniques-based PPP-SNC were used for antibacterial analysis against one gram-positive and one-gram negative

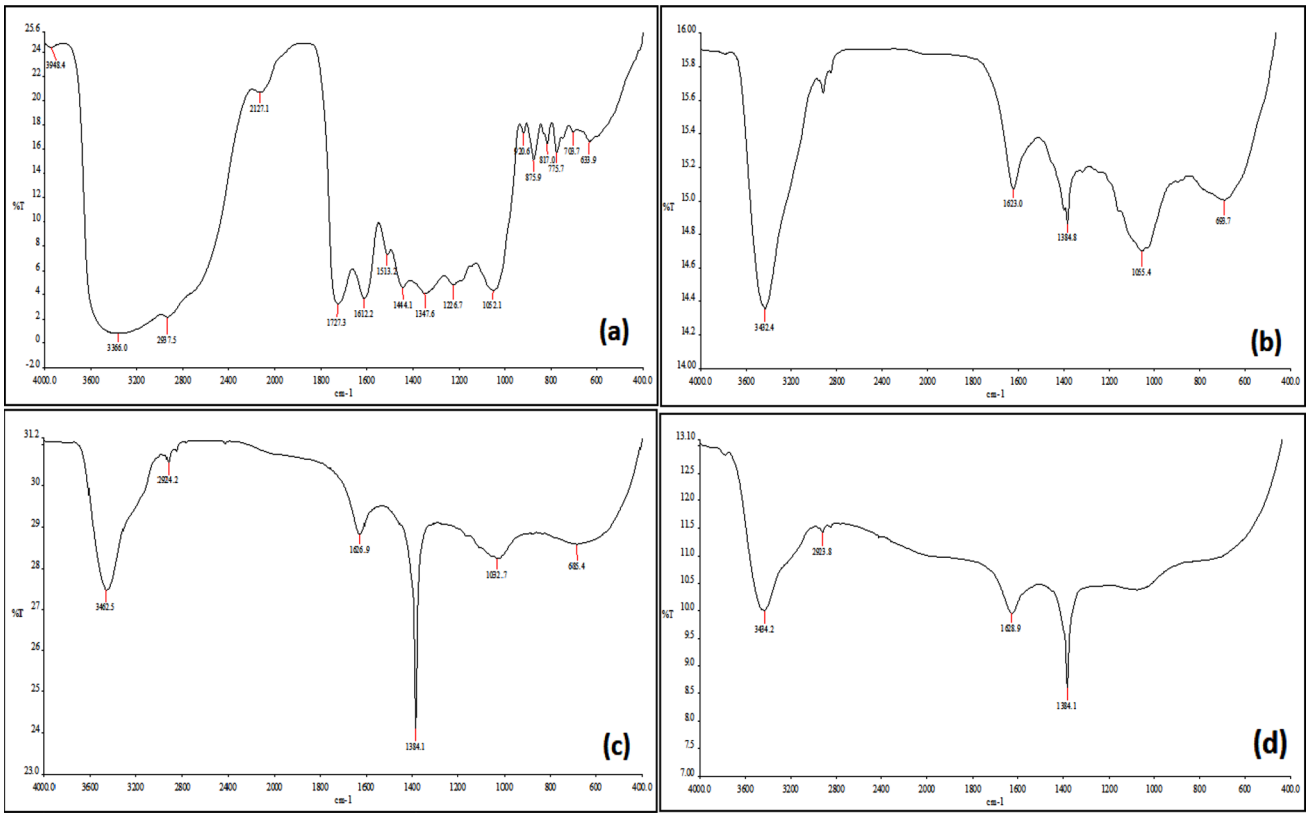

Fig. 5 FT-IR spectra of **a** PPP, **b** sunlight, **c** probe ultrasonication and **d** microwave treated PPP-SNC

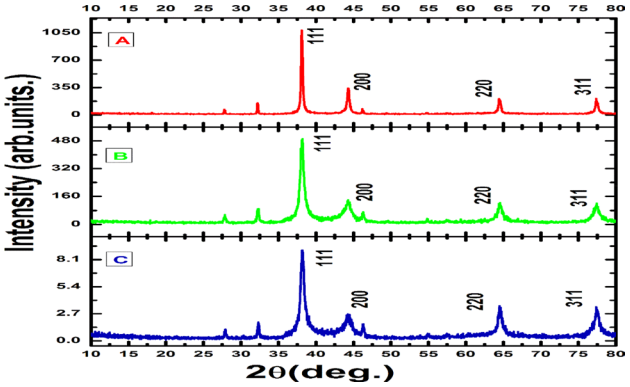

Fig. 6 XRD-spectra of **a** sunlight, **b** probe ultrasonication, and **c** microwave treated PPP-SNC

food pathogenic bacteria. The results of the antibacterial activity expressed as a zone of inhibition (mm) are shown in Fig. 12a–d and Table 6.

The zone of inhibition against *E. coli*. was larger than *S. aureus*. It may be due to the rigid cell wall structure of *S. aureus* (Gram-positive) which has a thick layer of peptidoglycan and composed of a linear chain of polysaccharides cross inked with small peptides [65, 66]. Probe ultrasonication assisted PPP-SNC showed the highest ZOI against both bacteria (Gram-positive and negative). But microwave-assisted PPP-SNC showed only ZOI against *E. coli*. The results could be explained by the fact that the antibacterial activity was dependent on the shape, size, and dose of synthesized nanoparticles [67, 68]. As discussed earlier, DLS results and TEM images, the particle size of nanoconjugates were smaller and evenly distributed in PPP-SNC synthesized by probe ultrasonic. Since smaller size relates to the increased surface area which could easily bind with the cell membrane of bacteria and damage the DNA and subsequent cell death. On another side, aggregated and larger particles with a lower dose of microwave irradiated PPP-SNC were not efficient to inhibit the growth of *S. aureus*. It may be due to less penetration of the silver nanoparticles into the rigid cell wall.

A comparison of the antibacterial activity of PPP-SNC with other metals nanoparticles has been represented in Table 7. It was explored that the PPP-SNC exhibits better antibacterial activity than other materials-based nanoparticles such as iron, zinc, copper, and gold [61, 69–74]. Apart from it, the antibacterial efficacy of pomegranate peel

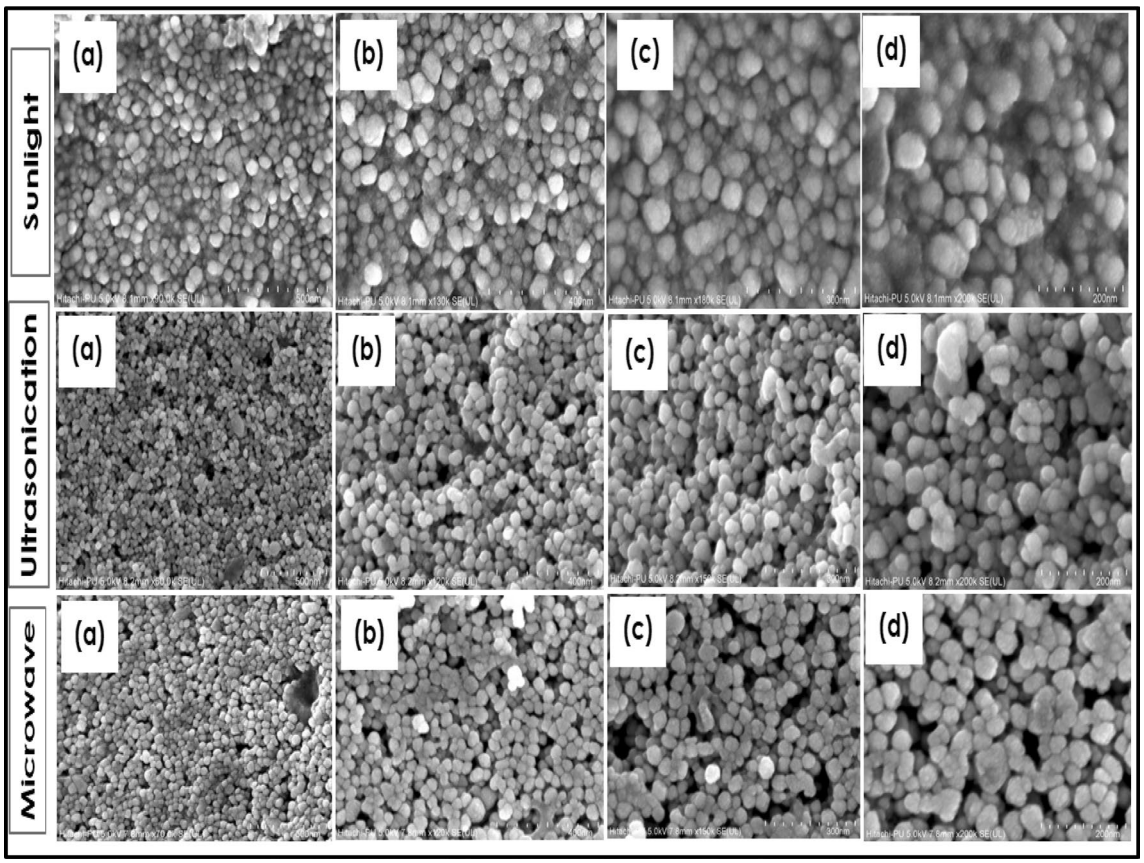

Fig. 7 FESEM images of PPE-SNC at **a** 500, **b** 400, **c** 300 and **d** 200 nm resolution

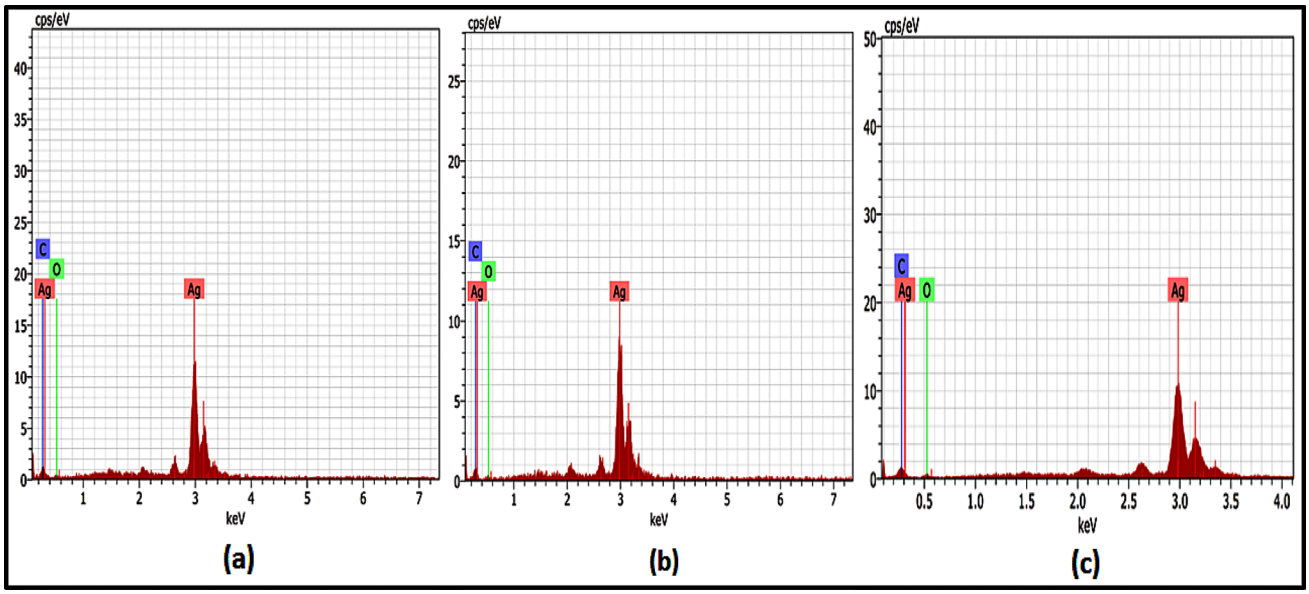

Fig. 8 EDX results of **a** sunlight, **b** probe ultrasonication, and **c** microwave treated PPP-SNC

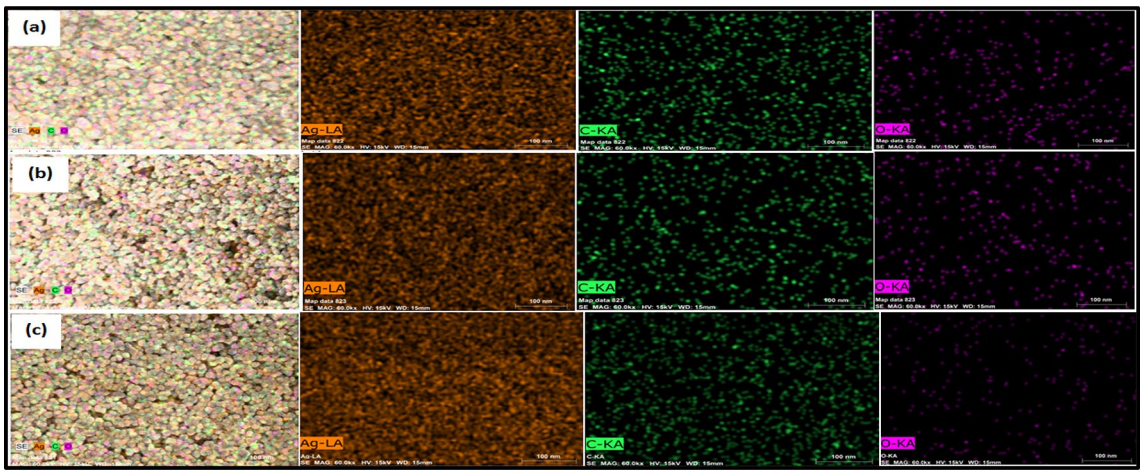

Fig. 9 Elemental mapping of **a** sunlight, **b** probe ultrasonication, and **c** microwave treated PPE-SNC

extract against *E. coli* and *S. aureus* was already studied and reported in our previous study [28]. The observations revealed that the extract at a concentration of 500 mg/ml showed ZOI 25 and 21 mm while the PPP-SNC at a concentration of 5 mg/ml showed 13.75 and 15.04 mm of ZOI against *S. aureus* and *E. coli*. This observation indicates that at the same concentration, the PPP-SNC will be exhibited higher antibacterial activity than PPP individually. Similar observation made by numerous studies [14, 24, 75].

Conclusion

Polyphenols from pomegranate peel were found capable to act as a capping and reducing agent for the synthesis of silver nanoparticles using sunlight, probe ultrasonication, and microwave irradiation. An enhanced yield, small spherical, and uniformly distributed PPP-SNC were

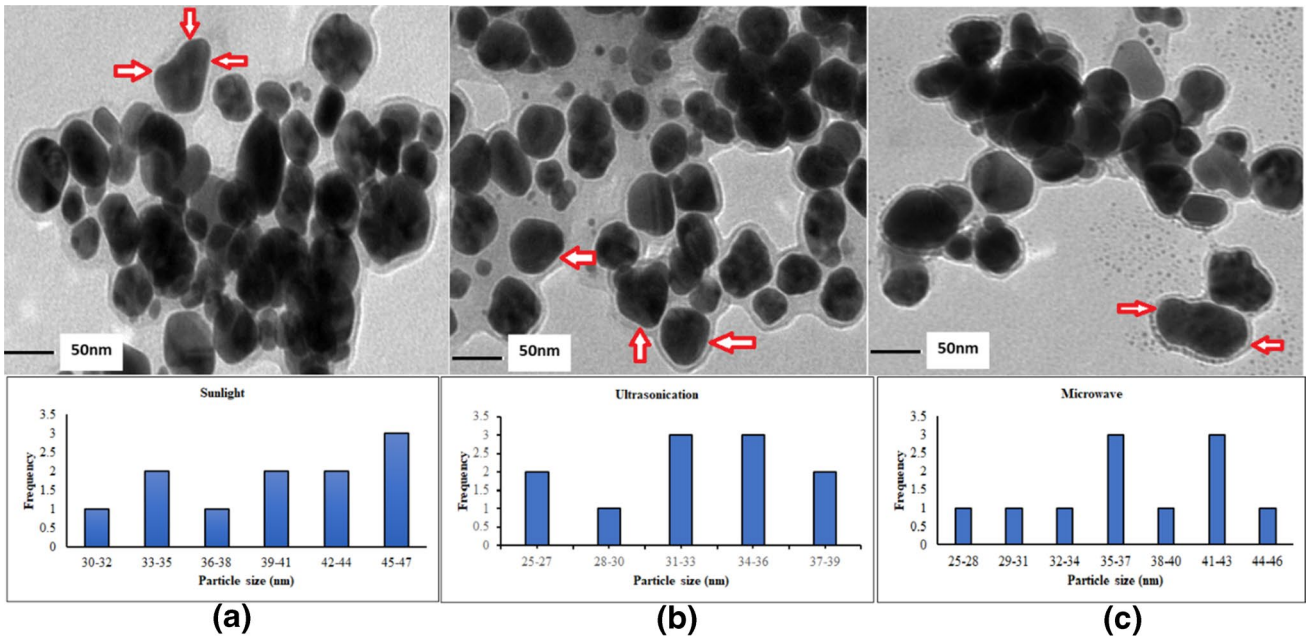

Fig. 10 TEM images with the histogram of **a** sunlight, **b** probe ultrasonication, and **c** microwave treated PPP-SNC. Highlighted red arrow indicates the presence of polyphenols as capping agent. (Color figure online)

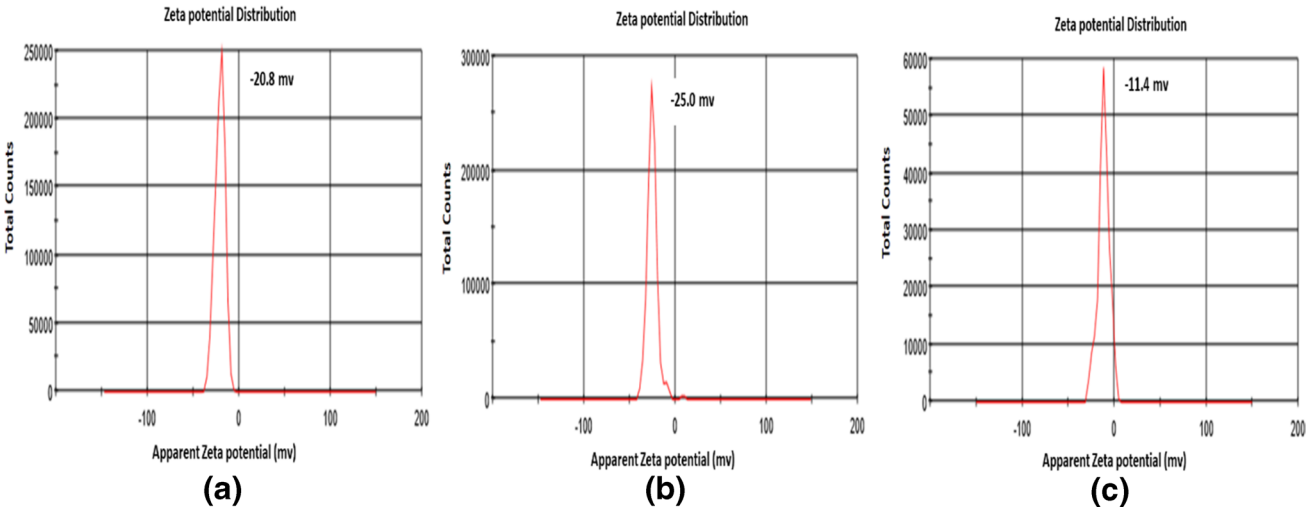

Fig. 11 Zeta potential (mv) of **a** sunlight, **b** probe ultrasonication, and **c** microwave treated PPP-SNC

obtained using probe ultrasonication at 40% of amplitude for 15 min in comparison to the other two approaches. FT-IR spectroscopy study provides clear evidence for the presence of polyphenols on the surface of silver nanoparticles. Antioxidant activity study showed that microwave irradiation and probe ultrasonication assisted PPP-SNC showed significantly enhanced antioxidant activity in comparison to sunlight assisted PPP-SNC. However, probe ultrasonication assisted PPP-SNC showed a good antibacterial activity at low concentration (50 µg/ml) against both gram-positive and negative bacteria. Therefore, probe ultrasonication-assisted greener-synthesis of

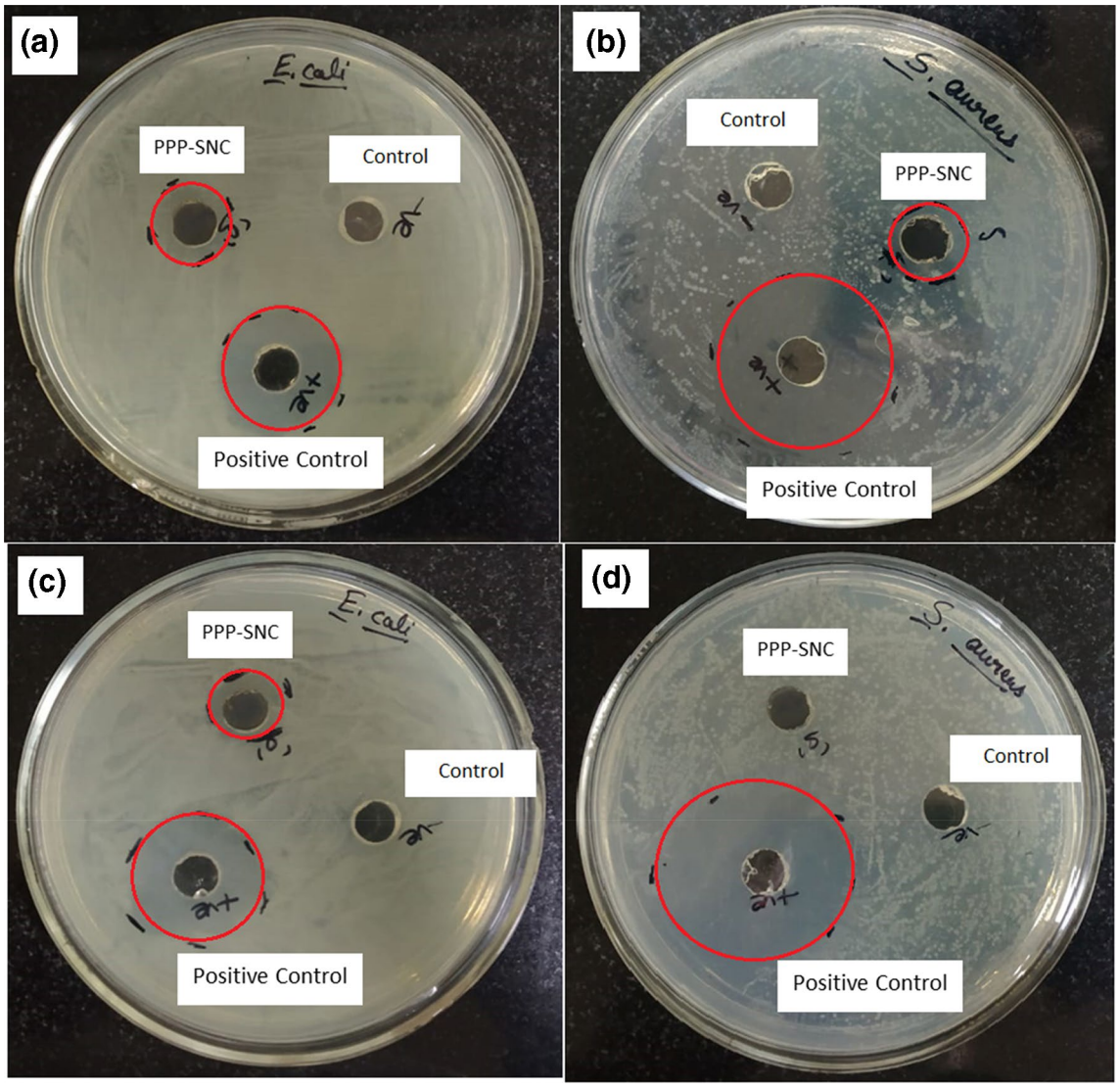

Fig. 12 Zone of inhibition of probe ultrasonic-assisted (**a**, **b**) and microwave-assisted PPP-SNC (**c**, **d**) against *E. coli* and *S. aureus*

Table 6 Antibacterial activity of PPP-SNC

No.	Sample	Zone of inhibition	
		E. coli	*S. aureus*
1	Control	No ZOI	No ZOI
2	Probe ultrasonication treated PPP-SNC (U)	15.04	13.75
3	Microwave treated PPP-SNC (M)	13.73	No ZOI
4	Tetracycline (positive control) (U-Petri plate)	24.44	32.92
5	Positive control (M-Petri plate)	24.27	32.72

silver is proved as a simple, eco-friendly, and efficient technique to produce a well structure-based smaller particle silver nanoconjugates. These nanoparticles will be delivered either in silver colloidal solution or dried powder form depends upon the type of application or intended uses. The emulsion-based nano colloidal silver can be used as a coating agent on the surface of fruit peels. The application of dried silver nanoparticles powder would subsidize as a filler in the biodegradable films to increase its tensile strength as well as provide protection against

Table 7 Comparative study of antibacterial activity of synthesized PPP-SNC with other material-based nanoparticles

Sl. no.	Metal nanoparticles	Sample concentration	Synthesis method	Size (nm)	ZOI (mm)		Refs.
					E. coli	*S. aureus*	
1	PPP-SNC	10 µl of 50 µg/ml	Probe-ultrasonication for 15 min	32 by TEM	15.04	13.75	Our study
2	Iron oxide (IO)	50 µg/disc	Co-precipitation	10–30 by TEM	8	–	[69]
3	IO + plant extracts	50 µg/disc	Shaking for 12 h	–	13	–	
4	*Psidium guajava*–IO	100 µg/ml	Stirrer for 1 h	1–6 by TEM	8	12	[70]
5	Sesame seed extract–zinc oxide (ZNO)	50 µg/ml	Sonication for 1 h	9.07 by XRD	3.7	No ZOI	[71]
6	*Berberis aristatata* extract–ZNO	100 µl of 100 mg/ml	Stirring until colour change	96 nm by DLS	13.0	–	[72]
7	*Agaricus-bisporus* extract – copper oxide (CuO)	100 µl of 30 µg/ml	Magnetic stirrer for 24 h	2–10 by TEM	8	–	[73]
8	CuO	100 µg/ml	Chemical	13.13 by TEM	5	–	[74]
9	Flavanoid tricitin–gold	100 µl of 500 µg/ml	–	12 nm by TEM	–	11.3	[61]

many food pathogens. The green synthesized PPP-SNC would contribute a significant role as antioxidant and antimicrobial in the field of food preservation including designing the novel food packaging system and postharvest management of fruits and vegetables. However, in the future, the study on cell cytotoxicity must be conducted to ascertain its safety use in various sectors.

Acknowledgements Financial support in the form of Institute fellowship from MHRD, New Delhi, India, technical assistance provided by the laboratory of sophisticated analytical instrumentation facility, Panjab University, Chandigarh and central laboratory of Punjab Agriculture University, Ludhiana for providing the facility of FESEM, LC-MS and TEM image analysis is gratefully acknowledged.

Funding Funding was provided by Ministry of Human Resource Development (Grant No. Dean(A)/Ph. D/8047).

Compliance with Ethical Standards

Conflict of interest The authors have no conflict of interest for this research article.

References

1. Nowack, B., Krug, H.F., Height, M.: 120 years of nanosilver history: implications for policy makers (2011). https://doi.org/10.1021/es103316q
2. Mittal, V.: Polymer layered silicate nanocomposites: a review. Materials **2**(3), 992–1057 (2009). https://doi.org/10.3390/ma2030992
3. Huang, Y., Mei, L., Chen, X., Wang, Q.: Recent developments in food packaging based on nanomaterials. Nanomaterials **8**(10), 830 (2018). https://doi.org/10.3390/nano8100830
4. Sreeram, K.J., Nidhin, M., Nair, B.U.: Microwave assisted template synthesis of silver nanoparticles. Bull. Mater. Sci. **31**(7), 937–942 (2008). https://doi.org/10.1007/s12034-008-0149-3
5. Goharshadi, E.K., Azizi-Toupkanloo, H.: Silver colloid nanoparticles: ultrasound-assisted synthesis, electrical and rheological properties. Powder Technol. **237**, 97–101 (2013). https://doi.org/10.1016/j.powtec.2012.12.059
6. Lu, Z., Meng, M., Jiang, Y., Xie, J.: UV-assisted in situ synthesis of silver nanoparticles on silk fibers for antibacterial applications. Colloids Surf. A **447**, 1–7 (2014). https://doi.org/10.1016/j.colsurfa.2014.01.064
7. Guzmán, M.G., Dille, J., Godet, S.: Synthesis of silver nanoparticles by chemical reduction method and their antibacterial activity. Int. J. Chem. Biomol. Eng. **2**(3), 104–111 (2009)
8. Miao, W., Chan, T.H.: Ionic-liquid-supported synthesis: a novel liquid-phase strategy for organic synthesis. Acc. Chem. Res. **39**(12), 897–908 (2006). https://doi.org/10.1021/ar030252f
9. Wang, S., Zhang, Y., Ma, H.L., Zhang, Q., Xu, W., Peng, J., Zhai, M.: Ionic-liquid-assisted facile synthesis of silver nanoparticle-reduced graphene oxide hybrids by gamma irradiation. Carbon **55**, 245–252 (2013). https://doi.org/10.1016/j.carbon.2012.12.033
10. Aygün, A., Gülbağça, F., Nas, M.S., Alma, M.H., Çalımlı, M.H., Ustaoglu, B., Şen, F.: Biological synthesis of silver nanoparticles using *Rheum ribes* and evaluation of their anticarcinogenic and antimicrobial potential: a novel approach in phytonanotechnology. J. Pharm. Biomed. Anal. **179**, 113012 (2020). https://doi.org/10.1016/j.jpba.2019.113012
11. Gomathi, A.C., Rajarathinam, S.X., Sadiq, A.M., Rajeshkumar, S.: Anticancer activity of silver nanoparticles synthesized using aqueous fruit shell extract of *Tamarindus indica* on MCF-7 human breast cancer cell line. J. Drug Deliv. Sci. Technol. **55**, 101376 (2020). https://doi.org/10.1016/j.jddst.2019.101376
12. Madivoli, E.S., Kareru, P.G., Gachanja, A.N., Mugo, S.M., Makhanu, D.S., Wanakai, S.I., Gavamukulya, Y.: Facile synthesis of silver nanoparticles using *Lantana trifolia* aqueous extracts and their antibacterial activity. J. Inorg. Organomet. Polym. Mater. (2020). https://doi.org/10.1007/s10904-019-01432-5
13. Ottoni, C.A., Lima Neto, M.C., Léo, P., Ortolan, B.D., Barbieri, E., De Souza, A.O.: Environmental impact of biogenic silver nanoparticles in soil and aquatic organisms. Chemosphere **239**, 124698 (2020). https://doi.org/10.1016/j.chemosphere.2019.124698

14. Hasnain, M.S., Javed, M.N., Alam, M.S., Rishishwar, P., Rishishwar, S., Ali, S., Beg, S.: Purple heart plant leaves extract-mediated silver nanoparticle synthesis: optimization by Box–Behnken design. Mater. Sci. Eng. C **99**, 1105–1114 (2019). https://doi.org/10.1016/j.msec.2019.02.061
15. Rautela, A., Rani, J., Das, M.D.: Green synthesis of silver nanoparticles from *Tectona grandis* seeds extract: characterization and mechanism of antimicrobial action on different microorganisms. J. Anal. Sci. Technol. **10**(1), 1–10 (2019). https://doi.org/10.1186/s40543-018-0163-z
16. Sowmiya, K., Prakash, J.T.J.: Green-synthesis of silver nanoparticles using *Abies webbiana* LEAVES and evaluation of its antibacterial activity. J. Pharmacogn. Phytochem. **7**(5), 2033–2036 (2018)
17. Shu, M., He, F., Li, Z., Zhu, X., Ma, Y., Zhou, Z., Yang, Z., Gao, F., Zeng, M.: Biosynthesis and antibacterial activity of silver nanoparticles using yeast extract as reducing and capping agents. Nanoscale Res. Lett. **15**(1), 14 (2020). https://doi.org/10.1186/s11671-019-3244-z
18. Foujdar, R., Bera, M.B., Chopra, H.K.: Phenolic nanoconjugates and its application in food. In: Biopolymer-Based Formulations, pp. 751–780. Elsevier (2020). https://doi.org/10.1016/B978-0-12-816897-4.00030-8
19. Jahan, I., Erci, F., Isildak, I.: Microwave-assisted green synthesis of non-cytotoxic silver nanoparticles using the aqueous extract of *Rosa santana* (rose) petals and their antimicrobial activity. Anal. Lett. **52**(12), 1860–1873 (2019). https://doi.org/10.1080/00032719.2019.1572179
20. Al-Nuairi, A.G., Mosa, K.A., Mohammad, M.G., El-Keblawy, A., Soliman, S., Alawadhi, H.: Biosynthesis, characterization, and evaluation of the cytotoxic effects of biologically synthesized silver nanoparticles from *Cyperus conglomeratus* root extracts on breast cancer cell line MCF-7. Biol. Trace Elem. Res. **194**(2), 560–569 (2020). https://doi.org/10.1007/s12011-019-01791-7
21. Khorrami, S., Zarrabi, A., Khaleghi, M., Danaei, M., Mozafari, M.R.: Selective cytotoxicity of green synthesized silver nanoparticles against the MCF-7 tumor cell line and their enhanced antioxidant and antimicrobial properties. Int. J. Nanomed. **13**, 8013 (2018). https://doi.org/10.2147/IJN.S189295
22. Senthil, B., Devasena, T., Prakash, B., Rajasekar, A.: Non-cytotoxic effect of green synthesized silver nanoparticles and its antibacterial activity. J. Photochem. Photobiol. B **177**, 1–7 (2017). https://doi.org/10.1016/j.jphotobiol.2017.10.010
23. Nasr, H.A., Nassar, O.M., El-Sayed, M.H., Kobisi, A.A.: Characterization and antimicrobial activity of lemon peel mediated green synthesis of silver nanoparticles. Int. J. Biol. Chem. **12**(2), 56–63 (2020). https://doi.org/10.26577/ijbch-2019-i2-7
24. Soto, K.M., Quezada-Cervantes, C.T., Hernández-Iturriaga, M., Luna-Bárcenas, G., Vazquez-Duhalt, R., Mendoza, S.: Fruit peels waste for the green synthesis of silver nanoparticles with antimicrobial activity against foodborne pathogens. LWT **103**, 293–300 (2019). https://doi.org/10.1016/j.lwt.2019.01.023
25. Kaviya, S., Santhanalakshmi, J., Viswanathan, B., Muthumary, J., Srinivasan, K.: Biosynthesis of silver nanoparticles using *Citrus sinensis* peel extract and its antibacterial activity. Spectrochim. Acta Part A Mol. Biomol. Spectrosc. **79**(3), 594–598 (2011). https://doi.org/10.1016/j.saa.2011.03.040
26. Tanase, C., Berta, L., Coman, N.A., Roşca, I., Man, A., Toma, F., Mare, A.: Investigation of in vitro antioxidant and antibacterial potential of silver nanoparticles obtained by biosynthesis using beech bark extract. Antioxidants **8**(10), 459 (2019). https://doi.org/10.3390/antiox8100459
27. Burlacu, E., Tanase, C., Coman, N.A., Berta, L.: A review of bark-extract-mediated green synthesis of metallic nanoparticles and their applications. Molecules **24**(23), 4354 (2019). https://doi.org/10.3390/molecules24234354
28. Foujdar, R., Bera, M.B., Chopra, H.K.: Optimization of process variables of probe ultrasonic-assisted extraction of phenolic compounds from the peel of *Punica granatum* Var. Bhagwa and it's chemical and bioactivity characterization. J. Food Process. Preserv. **44**(1), 14317 (2020). https://doi.org/10.1111/jfpp.14317
29. Ben-Ali, S., Akermi, A., Mabrouk, M., Ouederni, A.: Optimization of extraction process and chemical characterization of pomegranate peel extract. Chem. Pap. **72**(8), 2087–2100 (2018)
30. Ravichandran, V., Vasanthi, S., Shalini, S., Shah, S.A.A., Harish, R.: Green synthesis of silver nanoparticles using *Atrocarpus altilis* leaf extract and the study of their antimicrobial and antioxidant activity. Mater. Lett. **180**, 264–267 (2016). https://doi.org/10.1016/j.matlet.2016.05.172
31. Nasiriboroumand, M., Montazer, M., Barani, H.: Preparation and characterization of biocompatible silver nanoparticles using pomegranate peel extract. J. Photochem. Photobiol. B **179**, 98–104 (2018). https://doi.org/10.1016/j.jphotobiol.2018.01.006
32. Shanmugavadivu, M., Kuppusamy, S., Ranjithkumar, R.: Synthesis of pomegranate peel extract mediated silver nanoparticles and its antibacterial activity. Am. J. Adv. Drug Deliv. **2**(2), 174–182 (2014)
33. Deshmukh, A.R., Gupta, A., Kim, B.S.: Ultrasound assisted green synthesis of silver and iron oxide nanoparticles using fenugreek seed extract and their enhanced antibacterial and antioxidant activities. Biomed. Res. Int. (2019). https://doi.org/10.1155/2019/171435
34. Jayapriya, M., Dhanasekaran, D., Arulmozhi, M., Nandhakumar, E., Senthilkumar, N., Sureshkumar, K.: Green synthesis of silver nanoparticles using *Piper longum* catkin extract irradiated by sunlight: antibacterial and catalytic activity. Res. Chem. Intermed. **45**(6), 3617–3631 (2019). https://doi.org/10.1007/s11164-019-03812-5
35. Seku, K., Gangapuram, B.R., Pejjai, B., Kadimpati, K.K., Golla, N.: Microwave-assisted synthesis of silver nanoparticles and their application in catalytic, antibacterial and antioxidant activities. J. Nanostruct. Chem. **8**(2), 179–188 (2018). https://doi.org/10.1007/s40097-018-0264-7
36. De Matteis, V., Rizzello, L., Ingrosso, C., Liatsi-Douvitsa, E., De Giorgi, M.L., De Matteis, G., Rinaldi, R.: Cultivar-dependent anticancer and antibacterial properties of silver nanoparticles synthesized using leaves of different olea europaea trees. Nanomaterials **9**(11), 1544 (2019). https://doi.org/10.3390/nano9111544
37. El-Batal, A.I., Gharib, F.A.E.L., Ghazi, S.M., Hegazi, A.Z., Hafz, A.G.M.A.E.: Physiological responses of two varieties of common bean (*Phaseolus vulgaris* L.) to foliar application of silver nanoparticles. Nanomater. Nanotechnol. **6**, 13 (2016). https://doi.org/10.5772/62202
38. Seeram, N., Lee, R., Hardy, M., Heber, D.: Rapid large-scale purification of ellagitannins from pomegranate husk, a by-product of the commercial juice industry. Sep. Purif. Technol. **41**(1), 49–55 (2005). https://doi.org/10.1016/j.seppur.2004.04.003
39. Yisimayili, Z., Abdulla, R., Tian, Q., Wang, Y., Chen, M., Sun, Z., Huang, C.: A comprehensive study of pomegranate flowers polyphenols and metabolites in rat biological samples by high-performance liquid chromatography quadrupole time-of-flight mass spectrometry. J. Chromatogr. A **1604**, 460472 (2019). https://doi.org/10.1016/j.chroma.2019.460472
40. Fischer, U.A., Carle, R., Kammerer, D.R.: Identification and quantification of phenolic compounds from pomegranate (*Punica granatum* L.) peel, mesocarp, aril and differently produced juices by HPLC-DAD–ESI/MSn. Food Chem. **127**(2), 807–821 (2011). https://doi.org/10.1016/j.foodchem.2010.12.156

41. Mena, P., Calani, L., Dall'Asta, C., Galaverna, G., García-Viguera, C., Bruni, R., Del Rio, D.: Rapid and comprehensive evaluation of (poly) phenolic compounds in pomegranate (*Punica granatum* L.) juice by UHPLC-MSn. Molecules **17**(12), 14821–14840 (2012). https://doi.org/10.3390/molecules171214821
42. Preethi, P., Padma, P.R.: Biocompatibility of biosynthesized silver nano bio conjugates derived from a methanolic extract of *Piper betle* leaves. Indo Am. J. Pharm. Res. **6**, 5661–5670 (2016)
43. Kazemi, M., Karim, R., Mirhosseini, H., Hamid, A.A.: Optimization of pulsed ultrasound-assisted technique for extraction of phenolics from pomegranate peel of Malas variety: punicalagin and hydroxybenzoic acids. Food Chem. **206**, 156–166 (2016). https://doi.org/10.1016/j.foodchem.2016.03.017
44. Mahajan, P., Sharma, A., Kaur, B., Goyal, N., Gautam, S.: Green synthesized (*Ocimum sanctum* and *Allium sativum*) Ag-doped cobalt ferrite nanoparticles for antibacterial application. Vacuum **161**, 389–397 (2019)
45. Pawar, J.S., Patil, R.H.: Green synthesis of silver nanoparticles using *Eulophia herbacea* (Lindl.) tuber extract and evaluation of its biological and catalytic activity. SN Appl. Sci. **2**(1), 52 (2020). https://doi.org/10.1007/s42452-019-1846-9
46. Baidukova, O., Skorb, E.V.: Ultrasound-assisted synthesis of magnesium hydroxide nanoparticles from magnesium. Ultrason. Sonochem. **31**, 423–428 (2016). https://doi.org/10.1016/j.ultsonch.2016.01.034
47. Khan, M.J., Kumari, S., Shameli, K., Selamat, J., Sazili, A.Q.: Green synthesis and characterization of pullulan mediated silver nanoparticles through ultraviolet irradiation. Materials **12**(15), 2382 (2019). https://doi.org/10.3390/ma12152382
48. Khan, M.J., Shameli, K., Sazili, A.Q., Selamat, J., Kumari, S.: Rapid green synthesis and characterization of silver nanoparticles arbitrated by curcumin in an alkaline medium. Molecules **24**(4), 719 (2019). https://doi.org/10.3390/molecules24040719
49. Sana, S.S., Dogiparthi, L.K.: Green synthesis of silver nanoparticles using *Givotia moluccana* leaf extract and evaluation of their antimicrobial activity. Mater. Lett. **226**, 47–51 (2018). https://doi.org/10.1016/j.matlet.2018.05.009
50. Fatimah, I.: Green synthesis of silver nanoparticles using extract of *Parkia speciosa* Hassk pods assisted by microwave irradiation. J. Adv. Res. **7**(6), 961–969 (2016). https://doi.org/10.1016/j.jare.2016.10.002
51. Fatimah, I., Indriani, N.: Silver nanoparticles synthesized using *Lantana camara* flower extract by reflux, microwave and ultrasound methods. Chem. J. Moldova **13**(1), 95–102 (2018). https://doi.org/10.19261/cjm.2017.461
52. Park, M., Sohn, Y., Shin, W.G., Lee, J., Ko, S.H.: Ultrasonication assisted production of silver nanowires with low aspect ratio and their optical properties. Ultrason. Sonochem. **22**, 35–40 (2015). https://doi.org/10.1016/j.ultsonch.2014.05.007
53. Yin, H., Yamamoto, T., Wada, Y., Yanagida, S.: Large-scale and size-controlled synthesis of silver nanoparticles under microwave irradiation. Mater. Chem. Phys. **83**(1), 66–70 (2004). https://doi.org/10.1016/j.matchemphys.2003.09.006
54. Kazemzadeh, S.M., Hassanjani-Roshan, A., Vaezi, M.R., Shokuhfar, A.: The effect of microwave irradiation time on appearance properties of silver nanoparticles. Trans. Indian Inst. Met. **64**(3), 261–264 (2011). https://doi.org/10.1007/s12666-011-0053-1
55. Kumar, B., Smita, K., Cumbal, L., Debut, A.: *Ficus carica* (Fig) fruit mediated green synthesis of silver nanoparticles and its antioxidant activity: a comparison of thermal and probe ultrasonication approach. BioNanoScience **6**(1), 15–21 (2016). https://doi.org/10.1007/s12668-016-0193-1
56. Ma, G.Z., Wang, C.M., Li, L., Ding, N., Gao, X.L.: Effect of pomegranate peel polyphenols on human prostate cancer PC-3 cells in vivo. Food Sci. Biotechnol. **24**(5), 1887–1892 (2015). https://doi.org/10.1007/s10068-015-0247-0
57. Mahendran, G., Kumari, B.R.: Biological activities of silver nanoparticles from *Nothapodytes nimmoniana* (Graham) Mabb. fruit extracts. Food Sci. Hum. Wellness **5**(4), 207–218 (2016). https://doi.org/10.1016/j.fshw.2016.10.001
58. Dipankar, C., Murugan, S.: The green synthesis, characterization and evaluation of the biological activities of silver nanoparticles synthesized from *Iresine herbstii* leaf aqueous extracts. Colloids Surf. B **98**, 112–119 (2012). https://doi.org/10.1016/j.colsurfb.2012.04.006
59. Mittal, A.K., Bhaumik, J., Kumar, S., Banerjee, U.C.: Biosynthesis of silver nanoparticles: elucidation of prospective mechanism and therapeutic potential. J. Colloid Interface Sci. **415**, 39–47 (2014). https://doi.org/10.1016/j.jcis.2013.10.018
60. Reddy, N.J., Vali, D.N., Rani, M., Rani, S.S.: Evaluation of antioxidant, antibacterial and cytotoxic effects of green synthesized silver nanoparticles by *Piper longum* fruit. Mater. Sci. Eng. C **34**, 115–122 (2014). https://doi.org/10.1016/j.msec.2013.08.039
61. Alsamhary, K., Al-Enazi, N., Alshehri, W.A., Ameen, F.: Gold nanoparticles synthesised by flavonoid tricetin as a potential antibacterial nanomedicine to treat respiratory infections causing opportunistic bacterial pathogens. Microb. Pathog. **139**, 103928 (2020). https://doi.org/10.1016/j.micpath.2019.103928
62. Bakhshandeh, R., Shafiekhani, A.: Ultrasonic waves and temperature effects on graphene structure fabricated by electrochemical exfoliation method. Mater. Chem. Phys. **212**, 95–102 (2018). https://doi.org/10.1016/j.matchemphys.2018.03.004
63. Klinkaewnarong, J., Utara, S.: Ultrasonic-assisted conversion of limestone into needle-like hydroxyapatite nanoparticles. Ultrason. Sonochem. **46**, 18–25 (2018). https://doi.org/10.1016/j.ultsonch.2018.04.002
64. Nikolaev, A.L., Gopin, A.V., Severin, A.V., Rudin, V.N., Mironov, M.A., Dezhkunov, N.V.: Ultrasonic synthesis of hydroxyapatite in non-cavitation and cavitation modes. Ultrason. Sonochem. **44**, 390–397 (2018). https://doi.org/10.1016/j.ultsonch.2018.02.047
65. Gopinath, V., MubarakAli, D., Priyadarshini, S., Priyadharsshini, N.M., Thajuddin, N., Velusamy, P.: Biosynthesis of silver nanoparticles from *Tribulus terrestris* and its antimicrobial activity: a novel biological approach. Colloids Surf. B **96**, 69–74 (2012). https://doi.org/10.1016/j.colsurfb.2012.03.023
66. Shrivastava, S., Bera, T., Roy, A., Singh, G., Ramachandrarao, P., Dash, D.: Characterization of enhanced antibacterial effects of novel silver nanoparticles. Nanotechnology **18**(22), 225103 (2007). https://doi.org/10.1088/0957-4484/18/22/225103
67. Girón-Vázquez, N.G., Gómez-Gutiérrez, C.M., Soto-Robles, C.A., Nava, O., Lugo-Medina, E., Castrejón-Sánchez, V.H., Luque, P.A.: Study of the effect of Persea americana seed in the green synthesis of silver nanoparticles and their antimicrobial properties. Results Phys. **13**, 102142 (2019). https://doi.org/10.1016/j.rinp.2019.02.078
68. López-Esparza, J., Espinosa-Cristóbal, L.F., Donohue-Cornejo, A., Reyes-López, S.Y.: Antimicrobial activity of silver nanoparticles in polycaprolactone nanofibers against gram-positive and gram-negative bacteria. Ind. Eng. Chem. Res. **55**(49), 12532–12538 (2016). https://doi.org/10.1021/acs.iecr.6b02300
69. Arokiyaraj, S., Saravanan, M., Prakash, N.U., Arasu, M.V., Vijayakumar, B., Vincent, S.: Enhanced antibacterial activity of iron oxide magnetic nanoparticles treated with *Argemone mexicana* L. leaf extract: an in vitro study. Mater. Res. Bull. **48**(9), 3323–3327 (2013). https://doi.org/10.1016/j.materresbull.2013.05.059
70. Madubuonu, N., Aisida, S.O., Ahmad, I., Botha, S., Zhao, T.K., Maaza, M., Ezema, F.I.: Bio-inspired iron oxide nanoparticles using *Psidium guajava* aqueous extract for antibacterial activity. Appl. Phys. A **126**(1), 1–8 (2020). https://doi.org/10.1007/s00339-019-3249-6
71. Zafar, S., Ashraf, A., Ijaz, M.U., Muzammil, S., Siddique, M.H., Afzal, S., Mahboob, S.: Eco-friendly synthesis of antibacterial

zinc nanoparticles using *Sesamum indicum* L. extract. J. King Saud Univ. Sci. **32**(1), 1116–1122 (2020). https://doi.org/10.1016/j.jksus.2019.10.017
72. Chandra, H., Patel, D., Kumari, P., Jangwan, J.S., Yadav, S.: Phyto-mediated synthesis of zinc oxide nanoparticles of *Berberis aristata*: characterization, antioxidant activity and antibacterial activity with special reference to urinary tract pathogens. Mater. Sci. Eng. C **102**, 212–220 (2019). https://doi.org/10.1016/j.msec.2019.04.035
73. Sriramulu, M., Shanmugam, S., Ponnusamy, V.K.: *Agaricus bisporus* mediated biosynthesis of copper nanoparticles and its biological effects: an in-vitro study. Colloid Interface Sci. Commun. **35**, 100254 (2020). https://doi.org/10.1016/j.colcom.2020.100254
74. Chaudhary, J., Tailor, G., Yadav, B.L., Michael, O.: Synthesis and biological function of Nickel and Copper nanoparticles. Heliyon **5**(6), e01878 (2019). https://doi.org/10.1016/j.heliyon.2019.e01878
75. Salari, S., Bahabadi, S.E., Samzadeh-Kermani, A., Yosefzaei, F.: In-vitro evaluation of antioxidant and antibacterial potential of greensynthesized silver nanoparticles using *Prosopis farcta* fruit extract. Iran. J. Pharm. Res. IJPR **18**(1), 430 (2019). https://www.ncbi.nlm.nih.gov/pmc/articles/pmc6487442/